

# Research on Mechanically Reconfigurable Reflectarray Antenna

Ao HU<sup>†</sup>, Keisuke KONNO<sup>†</sup>, and Qiang CHEN<sup>†</sup>

<sup>†</sup> Dept. of Communications Engineering, Graduate School of Engineering, Tohoku University,  
Aoba-ku, Sendai 980–8579, Japan

E-mail: thu.ao.p7@dc.tohoku.ac.jp

**Abstract** This paper addresses the advantages of mechanically reconfigurable reflectarray (RA) antenna compared to conventional RA. Two innovative ways of realizing mechanically reconfigurable RA antenna is proposed: electromagnets-controlled RA and rotatable cylinder RA. For electromagnets-controlled RA, A novel mechanically reconfigurable RA element actuated by an electromagnet working in C-band is proposed. 1-Bit phase shift of reflecting wave is achieved by bending a half-wavelength dipole with magnetostatic force. For rotatable cylinder RA, a low-cost approach for the design of mechanically phase-tunable RA elements operating in the C-band is proposed. The proposed element composes of an open cylindrical shell made of a non-uniform dielectric material. A 2-bit phase tunability is achieved by implementing mechanical rotation of the open cylindrical shell.

**Key words** Reflectarrays, on- off- control, electromagnet, additive manufacturing, antennas, arrays.

## 1. Introduction

A reflectarray (RA) antenna is a class of reflector antennas, which are composed of numerous reflecting elements, a primary source and a ground plane. The reflecting elements are typically designed so that the scattering wave from the reflecting elements is in-phase at a specific direction. By tuning the reflection coefficient phase and magnitude simultaneously for each element, the RA antenna is able to scan or form specific main beam. The first RA antenna is composed of an array of variable-length waveguides [1]. Although the first RA antenna is bulky and heavy, owing to the advancement of wireless communication systems, various planar RAs have been extensively studied due to their low-profile and high gain features [2]–[4].

Numerous applications were developed of RA, due to its important features such as high-gain, low-profile, simple feed and low-cost features. It is known that RA is compatible with the flat surface on the space craft. Therefore, it is a good substitution of parabolic antenna, which can save the valuable space on the satellite and exploration rover. In previous studies, the RAs were also developed for various applications in wireless communication system. In particular, the passive RAs have been applied to eliminate blindness of the wireless communication systems. A RA composed of non-identical planar dipole elements with parasitic elements was developed to eliminate blindness in a CDMA (WCDMA) communication system [5]. Two RAs whose reflecting surface were perpendicular to each other was proposed to improve signal coverage in a cornered corridor [6]. A RA composed of groove shaped elements was developed so that it can guide the incident field to the end-fire direction of the RA surface [7]. Although the passive RAs have capability to eliminate the blindness, their performance is not tunable once they are fabricated.

Mechanically reconfigurable RA using actuators or motors is an promising approach for designing the reconfigurable RA. Notable examples of mechanically reconfigurable RAs in-

clude variations in the height of patch elements [8] [9], bending a dipole strip element using electromagnet [10], rotation of specific parts of the reflecting elements [11]–[13], and the controlled deformation of flexible element through squeezing [14]. While mechanically reconfigurable RAs offer continuous phase shift, low-speed reconfigurability of the mechanical systems and high fabrication cost due to multiple number of actuators/motors or complicated shape of the RA elements are major disadvantages. To reduce the fabrication cost of the mechanically reconfigurable RAs, various RAs with the small number of actuators have been developed. For instance, a deformable ground plane actuated by only four motors was introduced [15]. A beam scanning RA by rotating the whole RA, not each RA element by single motor was proposed [16]. A beam scanning RA by actuating cascading elements using Archimedean spiral cam with single motor was designed [17]. Although the advancements on reducing fabrication cost are found, the cost-effective fabrication technologies for complicated shape of the RA elements are expected to be developed.

## 2. Electromagnet-controlled RA

The phase tuning mechanism is based on the height-tunable resonator approach [19]. The flexible copper strip over the elastic polystyrene film is flat when the electromagnet turns off, which forms a straight half-wavelength dipole over ground plane. Once the electromagnet turns on, the square steel patch underneath the center of the copper strip is attracted to the ground plane by the magnetostatic force, which then forms a bent dipole over ground plane. Such deformation and height tunability of the dipole element result in difference of electromagnetic response, i.e. phase of reflection coefficient [8]. Simulation results in the next subsection demonstrate the difference of electromagnetic response between straight/bent dipole elements. The attracting force is generated from magnetic coupling between the electromagnets and the steel patch via static magnetic field penetrating

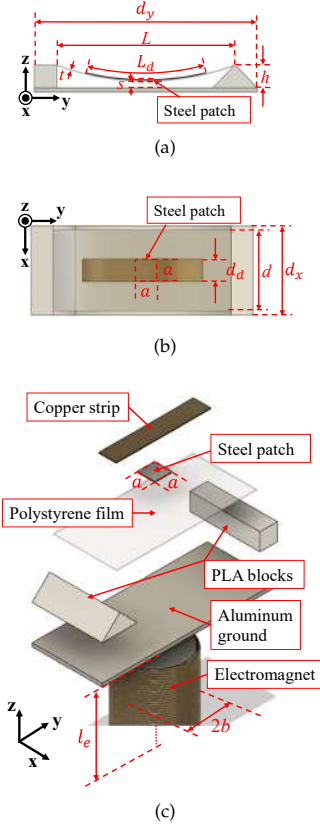


Fig. 1 The demonstration of electromagnet-controlled RA element (a). Side view, (b). Top view and (c). Birds eye view.

the ground plane. Although the magnetostatic field penetrates the ground plane, RF signals are shielded by the ground plane. Therefore, complete RF isolation between the RA element and the electromagnet (i.e., RF phase shifter) is achievable by the proposed RA element. As a result, the proposed RA element is free of insertion-loss of the RF phase shifter.

Scattering performance of the electromagnet controlled RA element under two-dimensional periodic boundary condition (PBC) is simulated by method of moments (MoM) using commercial simulator software FEKO. The working frequency of proposed electromagnet-controlled RA element is 4.4 GHz. Array spacing is  $d_x = 20$  mm ( $0.293\lambda$ ) and  $d_y = 50$  mm ( $0.733\lambda$ ), respectively. Dimensions of the RA element here are optimized ones according to the mechanical performance analysis shown in section II-C. Variation of reflection coefficient with respect to height  $s$  is shown in Fig. 2. It is found that  $180^\circ$  phase shift is available for two different angle of incidence  $(\theta_f, \varphi_f) = (0, 0^\circ), (30^\circ, 0)$  as  $s$  varies from 0 to 5 mm. Also, it is found that the drop of the magnitude is below 0.1 dB within the tunable range. The drop of the reflection magnitude stems from lossy dielectric material. According to the numerical results, it can be concluded that the proposed RA element meets the requirements of composing 1-bit reconfigurable RA.

A 1-bit  $25 \times 8$  elements RA is fabricated to demonstrate the beam scanning ability. The fabricated RA prototype is shown in Fig. 3a. Here, the fabricated RA prototype was designed to be large as much as possible so that it demonstrates high 1-bit resolution and superior beam scanning performance. As a result, aperture of the fabricated prototype is rectangular, not square because the largest available aluminum ground plane was rectangular one.

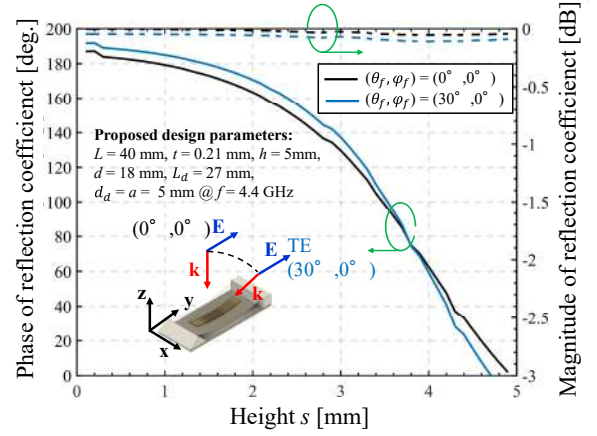


Fig. 2 Tunability of reflection coefficient with respect to height  $s$ .

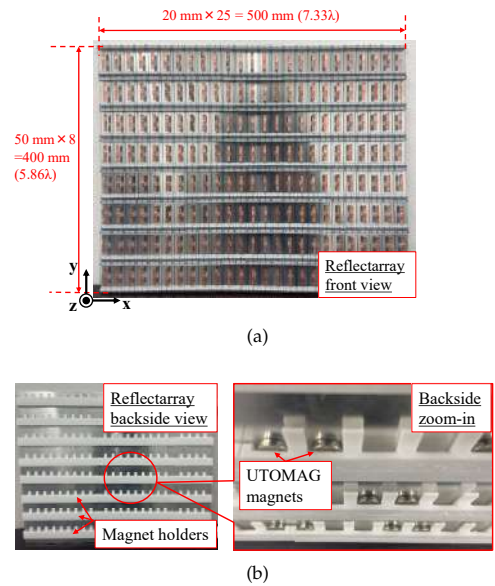


Fig. 3 Fabricated 1-bit  $25 \times 8$  (= 200) elements RA prototype (a) front view and (b) backside view. Here,  $\lambda$  is wavelength at  $f = 4.4$  GHz.

Permanent button magnets are used for tuning height of each RA element instead of the electromagnets to demonstrate the scattering performance of the proposed RA in a simple manner. UTOMAG  $12 \times 3$  mm magnet is chosen because when this magnet is attached close against the geometrical center behind the element ground plane, the steel patch can stably bend the dipole strip downward to achieve  $180^\circ$  phase shift. Because aluminum ground plane shields the backside structures from RF incident wave, electromagnets or button are isolated from the RA elements.

The RA backside view that behind ground plane is shown in Fig. 3b. 3-D printed magnet holders which can keep the positions of the button magnets are placed under the ground plane. As shown in right-hand side of Fig. 3b, the holders can hold the button magnets individually right under the geometrical center of each element. In this work, on-/off-state of the RA element is controlled by whether inserting a button magnet or not in the corresponding holder. The button magnets are inserted to the holder behind the on-state RA elements whereas they are not inserted to that behind the off-state RA elements.

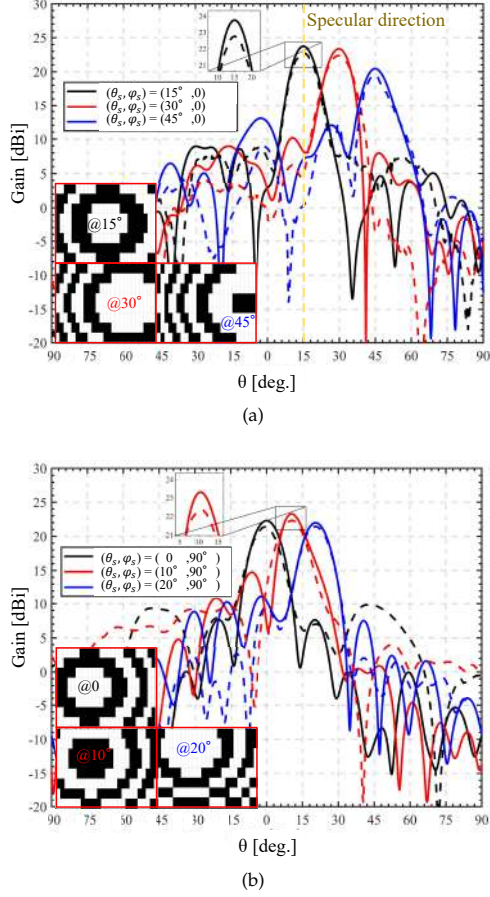


Fig. 4 Gain patterns of the proposed RA antennas at  $f = 4.4$  GHz for main beam directed in (a).  $xoz$ -plane ( $\varphi_s = 0$ ) and (b).  $yoz$ -plane ( $\varphi_s = 90^\circ$ ). The bold lines are simulation results obtained by FEKO, and the dashed lines are measurement results. On-states (white) and off-states (black) of the RA elements are shown in bottom-left.

Gain patterns of the proposed RA antenna are shown in Fig. 4. In the results, it is found that the measured main beam direction agrees well with those of simulated ones and two-dimensional beam scanning ability of the proposed RA antenna is demonstrated. For the scenario when RA antenna's main beam directed to specular direction ( $15^\circ, 0$ ), the measured gain is around 22.7 dBi, the first side-lobe level is -13.8 dB. Around 1 dB drop of the measured gain from the simulated one comes from material loss neglected in numerical simulation and the imperfect elimination of the reflection from the ground. As the main beam direction of the RA antenna approaches to  $\theta = 45^\circ$ , beam starts to distort, and a grating lobe appears at around  $(\theta, \varphi) = (5^\circ, 180^\circ)$ , because of the imperfect phase compensation by the 1-bit phase shift. The aperture efficiency of the RA antenna corresponding to specular reflection is 34.0%.

### 3. 3D-printed RA with Cylindrical elements

In this section, we propose a 2-bit 3D-printed RA element. The proposed element is composed of an open cylindrical shell of a dielectric material whose relative permittivity is non-uniform. Phase tunability of the proposed element is realized by rotating the open cylindrical shell mechanically. The open

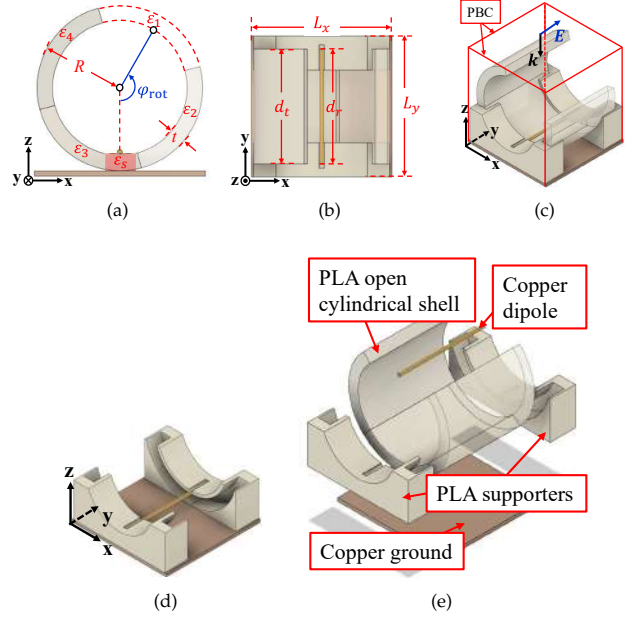


Fig. 5 The configuration of cylindrical RA element (a). Front view (Illustration of the PLA supporters are omitted here for visibility), (b). Top view, (c). Bird's eye view, (d) Bird's eye view with cylinder shell omitted and (e). Exploded view.

cylindrical shell is fabricated using the low-cost 3D-printed technology and non-uniform effective relative permittivity is achieved by printing non-uniform infill rate of material. Robust 2-bit phase tunability with respect to error of a rotation angle, which is an advantage of the proposed RA element, is demonstrated. The robust phase tunability contributes to reduce cost of mechanical control system because precise control of the rotation angle is unnecessary. Of course, the low-cost 3D-printed technology also contributes to reduce the fabrication cost.

A copper dipole with a length  $d_r$  fixed on PLA supporters is inside the open cylindrical shell, which is depicted in Fig. 5(d) in detail. In Fig. 5(d), the open cylindrical shell is omitted for enhancing visibility. The PLA supporters are slotted to support the dipole. The open cylindrical shell is freely rotatable around the dipole element because mechanical connection between them is absent. Rotation angle of the open cylindrical shell is denoted by  $\varphi_{rot}$ . Observing toward  $y$ -direction, the counter clock-wise rotation angle  $\varphi_{rot}$  is defined from the  $-z$ -direction to the blue line pointing to the center of vacuum part, as depicted in Fig. 5(a). Owing to the PLA supporters, position of the copper dipole is kept during rotation of the open cylindrical shell. Size of the copper ground in  $x$ -direction is  $L_x$  and that in  $y$ -direction is  $L_y$ .

The scattering performance of the proposed RA element was simulated under the periodic boundary condition (PBC) by the commercial simulator software FEKO based on the Method of Moments (MoM). Here, operating frequency of the RA element is 4.3 GHz and its array spacing in  $x$ - and  $y$ -directions are  $L_x = L_y = 33$  mm ( $0.473\lambda$ ). Amplitude variation and phase shift of the reflection coefficient along with the rotation angle  $\varphi_{rot}$  are demonstrated in Fig. 6. As the open cylindrical shell rotates, an obvious 2-bit staircase like phase shift was observed for reflection coefficients corresponding to all of the incident angles. According to phase shift of the

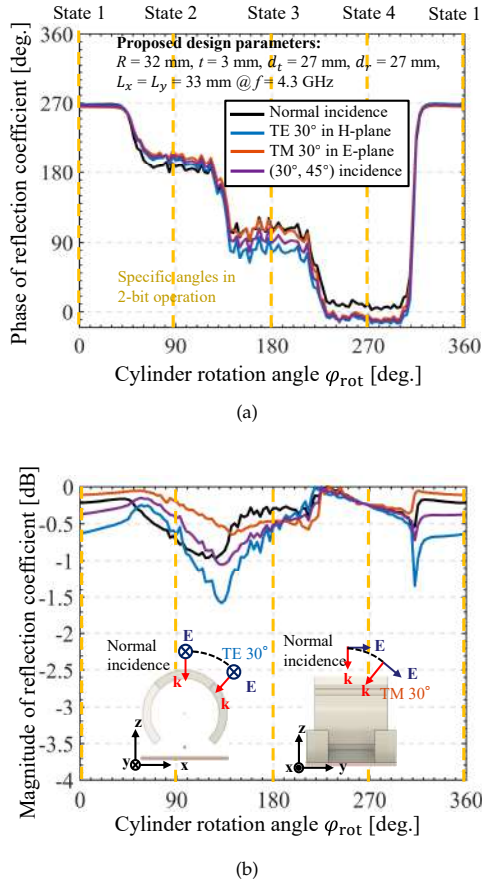


Fig. 6 Tunability of reflection coefficient with respect to open cylindrical shell rotation angle  $\varphi_{rot}$ . Specific angles of rotation corresponding to 2-bit operation are indicated by vertical yellow dashed lines.

reflection coefficient corresponding to incident angle  $(\theta, \varphi) = (30^\circ, 45^\circ)$ , whereas polarization is TE that E-field only has  $45^\circ \varphi$ -component, beam scanning capability outside E- and H- planes is expected to the RA using the proposed element. Small ripples appear on the phase shift because the reflection of reflection waves from fixed parts (i.e. dipole, supporters, and ground) and a rotated part (i.e. open cylindrical shell) of the RA element changes respectively due to mutual coupling as the open cylindrical shell rotates. The worst ripple on the phase shift is found around  $180^\circ$  and its level is approximately  $\pm 30^\circ$ . The level of the ripples is within  $\pm 45^\circ$  and can be tolerated for the 2-bit operation. The staircase like phase shift and the small level of the ripples within  $\pm 45^\circ$  contribute to the robust 2-bit phase tunability. As a result, requirements on accuracy of positioning of the open cylindrical shell are alleviated and high-speed rotation is achievable because rotation speed and accuracy is tradeoff. On the other hand, the magnitude drop of the reflection coefficient was at most 1.6 dB when the open cylindrical shell fully rotates. As for fixed angle in 2-bit operation, the magnitude drop was at most 0.8 dB. The observed magnitude drop stems from the loss of the PLA. According to the numerical results shown here, it is found that the proposed RA element demonstrates 2-bit phase shift with small loss less than 0.8 dB.

Fig. 7(a) shows a fabricated prototype of a planar RA with  $10 \times 10$  elements. The open cylindrical shells and their supporters were fabricated using the Flash Forge Guider 2s 3D printer. The fabricated RA is backed by a copper ground plane

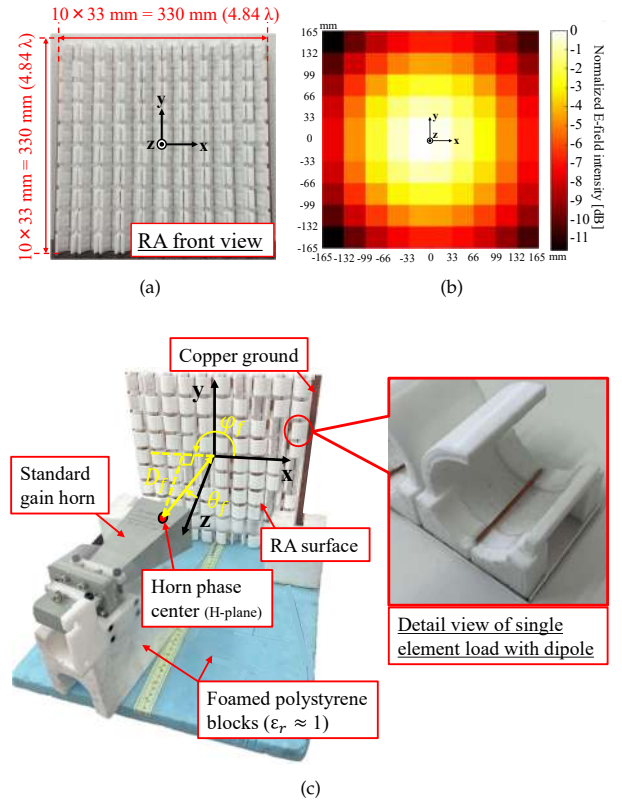


Fig. 7 Fabricated  $10 \times 10$  (= 100) elements RA antenna prototype (a). front view, (b) Illumination level over the RA surface and (c) RA illuminated by a horn antenna. Here,  $\lambda$  is wavelength at  $f = 4.3$  GHz.

and the dipole elements are made of copper wire with a diameter of 1 mm. A detailed view of single element is shown on the right-hand side in Fig. 7(c), where the dipole was inserted and taped in the slot of the PLA supporter so that their position is stationary as the open cylindrical shell rotates.

The gain patterns of the proposed RA antenna are demonstrated in Fig. 8. States of RA elements corresponding to main beam directions are shown in Fig. ???. In order to validate the measurement results, simulated results obtained using MoM are also shown in Fig. 8. Fig. 8 agreement between the measured gains and the simulated ones. For example, in the specular reflection scenario, where the main beam is steered to  $(\theta_s, \varphi_s) = (10^\circ, 0)$ , the gain reaches 20.2 dBi at maximum, with the first side-lobe level at -13.0 dB. On the other hand, as the main beam direction is steered to  $\theta_s = 50^\circ$ , the gain pattern distorts, and a grating lobe appears at around  $(\theta, \varphi) = (20^\circ, 180^\circ)$ . The distortion comes from error in phase compensation at large steering angle due to the effect of mutual coupling. Precise phase compensation over wide steering angle is a big challenge and future work. The aperture efficiency of the proposed RA antenna system in the specular reflection scenario is approximately 37.0%.

#### 4. Conclusion

The RA and RA antenna is a promising technology in 5G and upcoming 6G era. The low-profile, high-gain and simple feeding system feature of the RA allows it to be a good substitution of conventional parabolic antenna and phased array. The mechanical reconfigurable RA composes an important

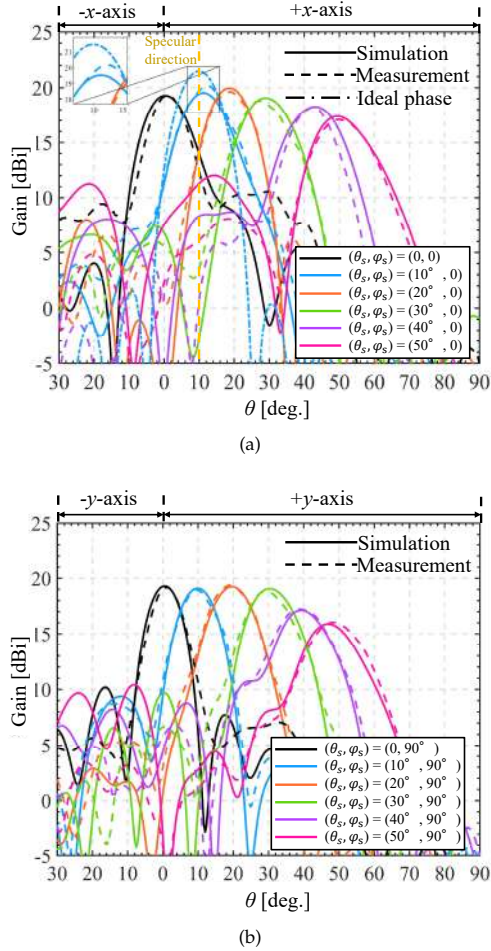


Fig. 8 Gain patterns of the proposed RA antenna at  $f = 4.3$  GHz for the main beam directed in (a).  $xoz$ -plane ( $\varphi_s = 0$ ), and (b).  $yo z$ -plane ( $\varphi_s = 90^\circ$ ). The solid lines represent the simulation results and the dashed lines represent the measurement results.

branch field of reconfigurable RA, whereas the mechanical solution to tuning the scattering characteristics of RA element has many advantages. This paper have demonstrated the high efficiency and low-cost feature of the mechanical reconfigurable RA through two novel approaches.

#### References

- [1] D.G. Berry, R.G. Malech, and W.A. Kennedy, "The reflectarray antenna", *IEEE Trans. Antennas Propag.*, vol. 11, no. 6, pp. 645-651, Nov. 1963.
- [2] J. Huang, "Analysis of a microstrip reflectarray antenna for microspacecraft applications," *TDA Progress Report 42-120*, pp. 153-173, Feb. 1995.
- [3] F. Yang and Y. Rahmat-Samii, *Surface Electromagnetics: With Applications in Antenna, Microwave, and Optical Engineering*, Cambridge, U.K.:Cambridge Univ. Press, Jun. 2019, doi:10.1017/9781108470261.
- [4] P. Nayeri, F. Yang and A.Z. Elsherbeni, *Reflectarray Antennas: Theory Designs and Applications*, John Wiley and Sons, 2018. doi:10.1002/9781118846728.
- [5] L. Li, Q. Chen, Q. Yuan, K. Sawaya, T. maruyama, T. Furuno, and S. Uebayashi, "Novel Broadband Planar Reflectarray With Parasitic Dipoles for Wireless Communication Applications," *IEEE Antennas Wireless Propag. Lett.*, vol. 8, pp. 881-885, 2009, doi: 10.1109/LAWP.2009.2028298.
- [6] P. Callaghan, P. Young and C. Gu, "Corner reflectarray

- for indoor wireless applications," in *Proc. Antennas and Propagation Conference 2019 (APC-2019)*, pp. 1-5, 2019, doi: 10.1049/cp.2019.0724.
- [7] D. Wang, R. Gillard and R. Loison, "A 60GHz passive repeater array with endfire radiation based on metal groove unit-cells," in *Proc. 2015 9th European Conference on Antennas and Propagation (EuCAP)*, pp.1-4, 2015.
- [8] X. Yang, S. Xu, F. Yang, M. Li, H. Fang, Y. Hou, S. Jiang and L. Liu, "A Mechanically Reconfigurable Reflectarray With Slotted Patches of Tunable Height," *IEEE Antennas Wireless Propag. Lett.*, vol. 17, no. 4, pp. 555-558, April 2018, doi: 10.1109/LAWP.2018.2802701.
- [9] J. P. Gianvittorio and Y. Rahmat-Samii, "Reconfigurable patch antennas for steerable reflectarray applications," *IEEE Trans. Antennas Propag.*, vol. 54, no. 5, pp. 1388-1392, May 2006, doi: 10.1109/TAP.2006.874311.
- [10] A. Hu, K. Konno, Q. Chen and T. Takahashi, "A Highly Efficient 1-bit Reflectarray Antenna Using Electromagnets-Controlled Elements," *IEEE Trans. Antennas Propag.*, vol. 72, no. 1, pp. 506-517, doi: 10.1109/TAP.2023.3324457.
- [11] V. F. Fusco, "Mechanical beam scanning reflectarray," *IEEE Trans. Antennas Propag.*, vol. 53, no. 11, pp. 3842-3844, Nov. 2005, doi: 10.1109/TAP.2005.858828.
- [12] X. Yang, S. Xu, F. Yang, M. Li, Y. Hou, S. Jiang, and L. Liu, "Broadband high-efficiency reconfigurable reflectarray antenna using mechanically rotational elements," *IEEE Trans. Antennas Propag.*, vol. 65, no. 8, pp. 3959-3966, Aug. 2017.
- [13] M. Wang, Y. Mo, W. Xie, N. Hu, Z. Chen and Z. Tian, "A 1-Bit All-Metal Wide-Angle and Multipolarization Beam-Scanning Reconfigurable Reflectarray Antenna," *IEEE Antennas Wireless Propag. Lett.*, vol. 22, no. 5, pp. 1015-1019, May 2023, doi: 10.1109/LAWP.2022.3230751.
- [14] Y. Cui, S. A. Nauroze, R. Bahr and E. M. Tentzeris, "3D Printed One-shot Deployable Flexible "Kirigami" Dielectric Reflectarray Antenna for mm-Wave Applications," in *Proc. 2020 IEEE/MTT-S International Microwave Symposium (IMS)*, pp. 1164-1167, 2020, doi: 10.1109/IMS30576.2020.9224010.
- [15] C. Benteyn, R. Gillard, E. Fourn, G. Goussetis, H. Legay and L. Datashvili, "A Design Methodology for Reconfigurable Reflectarrays with a Deformable Ground," in *Proc. 2020 14th European Conference on Antennas and Propagation (EuCAP)*, pp. 1-5, 2020, doi: 10.23919/EuCAP48036.2020.9135257.
- [16] M. I. Abbasi, M. H. Dahri, M. H. Jamaluddin, N. Seman, M. R. Kamarudin and N. H. Sulaiman, "Millimeter Wave Beam Steering Reflectarray Antenna Based on Mechanical Rotation of Array," *IEEE Access*, vol. 7, pp. 145685-145691, 2019, doi: 10.1109/ACCESS.2019.2945318.
- [17] Z. Cao, Y. Li, Z. Zhang and M. F. Iskander, "Single Motor-Controlled Mechanically Reconfigurable Reflectarray," *IEEE Trans. Antennas Propag.*, vol. 71, no. 1, pp. 190-199, Jan. 2023, doi: 10.1109/TAP.2022.3221036.
- [18] H. Yang, F. Yang, S. Xu, M. Li, J. Gao and Y. Zheng, "A Study of Phase Quantization Effects for Reconfigurable Reflectarray Antennas," *IEEE Antennas Wireless Propag. Lett.*, vol. 16, pp. 302-305, 2017, doi: 10.1109/LAWP.2016.2574118.
- [19] S. V. Hum and J. Perruisseau-Carrier, "Reconfigurable Reflectarrays and Array Lenses for Dynamic Antenna Beam Control: A Review," *IEEE Trans. Antennas Propag.*, vol. 62, no. 1, pp. 183-198, Jan. 2014, doi: 10.1109/TAP.2013.2287296.
- [20] **A. Hu**, K. Konno, Q. Chen and T. Takahashi, "A Highly Efficient 1-bit Reflectarray Antenna Using Electromagnet-Controlled Elements," *IEEE Trans. Antennas Propag.*, vol. 72, no. 1, pp. 506-517, Jan. 2024, doi: 10.1109/TAP.2023.3324457.